Volume complexity for the nonsupersymmetric Janus AdS_5 geometry

Stefano Baiguera,[*] Sara Bonansea,[†] and Kristian Toccacelo[‡]
The Niels Bohr Institute, University of Copenhagen, Blegdamsvej 17, DK-2100 Copenhagen Ø, Denmark

(Received 4 June 2021; accepted 30 September 2021; published 27 October 2021)

We compute holographic complexity for the nonsupersymmetric Janus deformation of AdS_5 according to the volume conjecture. The result is characterized by a power-law ultraviolet divergence. When a ball-shaped region located around the interface is considered, a subleading logarithmic divergent term and a finite part appear in the corresponding subregion volume complexity. Using two different prescriptions to regularize the divergences, we find that the coefficient of the logarithmic term is universal.

DOI: 10.1103/PhysRevD.104.086030

I. INTRODUCTION

A major role in the development of theoretical physics in the last decade was played by the AdS/CFT correspondence; the most studied example being the duality between $\mathcal{N}=4$ super Yang-Mills (SYM) theory with gauge group $SU(N)$ and type IIB string theory on $AdS_5 \times S^5$ [1]. While holography is a powerful tool in dealing with some particular physical systems, it is difficult to apply and test it in the strongly-coupled phase of gravity. An enormous improvement in the quantitative understanding of the correspondence has been possible thanks to the relationship between geometric objects in the bulk and information properties of quantum systems, starting from the duality between the entanglement entropy of a state on the boundary and the area of a codimension-two extremal surface [2]. It was recently argued that the evolution of the Einstein-Rosen Bridge (ERB) cannot be captured by entropy, since it grows for a much longer timescale compared to the thermalization time. For this reason, a new boundary quantity that supposedly encodes the information on the ERB has been introduced, that is, complexity. Two different gravity duals for computational complexity have been conjectured; the complexity = volume (CV) [3,4] and the complexity = action (CA) [5,6]. In the CV conjecture, complexity is proportional to the volume of a maximal codimension-one submanifold hanging from the boundary

$$\mathcal{C}_V = \frac{\mathcal{V}}{GL}, \tag{1.1}$$

where $\mathcal{V}$ is the above-mentioned volume, G is the Newton constant, and L is the anti–de Sitter (AdS) radius. In contrast, CA-duality relates the complexity on the boundary to the gravitational action I evaluated on the Wheeler-De Witt (WDW) patch, i.e., the bulk domain of dependence of a Cauchy surface anchored at the boundary

$$\mathcal{C}_A = \frac{I_{\mathrm{WDW}}}{\pi\hbar}. \tag{1.2}$$

One of the original motivations to formulate the action proposal was the universality of the definition, since it does not require the introduction of an *ad hoc* length scale. Early studies of the two conjectures for asymptotically AdS black holes have shown that the growth rate is the same at late times [6]. However, it was later found that the proposals have different behaviors at intermediate times [7,8]. Many attempts to distinguish volume from action have been made by studying the following scenarios; the complexity of formation of a black hole from empty AdS space [9], time-dependent spacetimes [10–12], cosmological models [13], backgrounds with nonrelativistic traits [14–16], higher-derivative gravity [17,18], and more.

Parallel developments from the boundary theory perspective have also taken place. Computational complexity is defined in quantum mechanics (QM) as the minimal number of simple[1] unitary operators that must be used to transform a reference state into a target state. This definition is well posed for discrete operators in quantum circuits, however, in view of the application to holography,

[*]stefano.baiguera@nbi.ku.dk
[†]sara.bonansea@nbi.ku.dk
[‡]btm438@alumni.ku.dk

[1]The term simple usually refers to operators which are k–local, i.e., operators that act on at most $k \in \mathbb{N}$ qubits at the same time. The typical choice is to consider two local operators, since it is the simplest action that creates a nonvanishing entanglement.

it is necessary to generalize the definition to the continuum case. A possible route was proposed by Nielsen *et al.* in [19]. Adopting Nielsen's approach, many advances have been made both from the QM and QFT point of view, such as the investigation of curvature properties of the unitary group [20], the relation between the spaces of unitaries and states in terms of Riemannian submersions [21], the application to the SYK model [22], the properties of geodesics for integrable and chaotic systems [23], the implementation in free theories [24–26], the proposal of a first law of complexity [27] and the application to conformal field theories (CFTs) [28,29]. A different avenue is that of path integral optimization [30,31].

An intriguing problem is the investigation of the UV divergences that arise in the computation of complexity for both sides of the duality. In the case of entanglement entropy, divergences occur as a consequence of the arbitrarily short correlations entangling the degrees of freedom in a subregion to the degrees of freedom in its complement. A general classification reveals that the leading divergence scales with an area law. Depending on the number of boundary dimensions, there is a universal term corresponding to the coefficient of the logarithmic divergence (even dimensions) or to the finite part (odd dimensions). Such terms are universal because they do not depend on rescalings of the UV regulator. This kind of general classification can also be done for the CV and CA conjectures, leading to the identification of the divergences in terms of curvature invariants integrated over a spatial slice [32,33]. There are two typical prescriptions to regularize the UV divergences in the action computation; they correspond to send the null geodesics defining the boundary of the WDW patch from the value $z = \delta$ along the radial direction of AdS space, or from the true boundary at $z = 0$, and cut them afterwards with a cutoff surface. It is meaningful to notice that the introduction of appropriate counterterms allows to find regularization-independent results, which is a step towards a universal classification of UV divergences in complexity [34,35].

In this paper, we analyze the structure of divergences and their universality properties in the case of CV-duality applied to a defect geometry. A defect is generally defined as a modification of a system localized on a submanifold. Conformal defects provide a useful tool to probe the dynamics of some theories [36–38]. Generally speaking, the insertion of a conformal defect in the vacuum of a theory results in the breaking of the full conformal group into a less constraining subgroup. Boundaries, defects, and interfaces have many applications both from a theoretical and phenomenological point of view. They constitute a simple path to bridge the gap between highly symmetric models studied in the context of the AdS/CFT duality and more physically realistic systems. For instance, condensed matter systems have impurities and, being finite in size, are also restricted by boundaries. Typical examples of defects are Wilson and 't Hooft operators in gauge theories [39,40] and D-branes in string theory. In high-energy physics, defects can be engineered holographically [41,42]. For example, the study of the CFT data associated to the $D3-D5$-brane system described in [43] was started in [44,45] and a plethora of subsequent studies have been carried out [46–53].

Furthermore, it is enticing to think of using defects as possible means to distinguish between the volume and the action proposals mentioned above. This route was taken in [54], where the CA and CV conjectures were inspected in the case of a bottom-up Randall-Sundrum type model [55] of a thin AdS_2 brane embedded in AdS_3 spacetime. The remarkable output of this analysis is that, for the CV proposal, a new logarithmic divergence appears in the holographic complexity due to the presence of the defect, whereas the action computation is unaffected. In [56,57], the holographic complexity was computed for a boundary CFT (BCFT). In particular, the analysis of [57] focuses on the gravitational dual of a boundary conformal field theory in two dimensions ($BCFT_2$). The authors found that the boundary distinguishes between CA and CV proposals in this case, too. In particular, a logarithmic divergence, whose coefficient depends on the boundary data, occurs in the CV computation. Instead, for CA this divergence drops out and the dependence on the boundary data occurs in the finite term. In [58], volume complexity was computed for a defect theory consisting of a Janus deformation of AdS_3 spacetime. It turns out that this setting admits precisely a logarithmic divergence whose coefficient is universal (i.e., independent of the regularization scheme and temperature of the configuration).

Nevertheless, in [56] it was pointed out that the result for $AdS_3/BCFT_2$ cannot be extended to higher dimensions, which is not surprising given that gravity is known to have special features in three dimensions. In fact, in higher dimensional cases, the boundary complexity is nonvanishing both in CV and CA conjectures, and only contains a power-law divergence which depends on the dimensionality of the spacetime.

In this paper, we focus on a nonsupersymmetric (non-SUSY) Janus deformation of AdS_5 spacetime to inspect the structure and the universality of UV divergences, in particular in comparison to the lower-dimensional case [58]. Volume complexity in the context of theories with defects was also recently studied in [59,60].

The paper is organized as follows. In Sec. II we describe the foliation of AdS_{d+1} space into AdS_d slices, which is useful to describe the defect geometry, and the properties of five-dimensional non-SUSY Janus spacetime. In Sec. III we compute the complexity of formation for the Janus deformation using two different regularization schemes. In Sec. IV we study the subregion complexity for a ball-shaped region centered on the defect using the same regularization procedures as for the total spacetime

computation. We comment on the universal structure of the UV divergences in the CV approach in Sec. V. An appendix about the Weierstrass $\wp$–function completes the paper.

II. FIVE-DIMENSIONAL JANUS ADS GEOMETRY

The non-SUSY Janus deformation of $AdS_5 \times S^5$ is a solution of type IIB supergravity with a nontrivial dilaton profile, which is regular and classically stable against all small and a certain class of large perturbations [61,62]. It can be thought of as a thick AdS_4-sliced domain wall in AdS_5. The CFT dual is given by the $\mathcal{N} = 4$ Super Yang-Mills (SYM) theory on both sides of a planar codimension-one interface, whose coupling constant varies discontinuously across the interface [63] where the half-spaces are glued together. The two different values of the gauge coupling correspond to the two asymptotic values of the dilaton in the Janus deformation. The SO(2,3) symmetry of the Janus geometry maps to the conformal group preserved by the three-dimensional interface on the CFT side. This symmetry is manifest at the classical level, but was also shown to persist at the first nontrivial quantum level [64]. The SO(6) symmetry of the Janus solution maps to an (accidental) internal symmetry[2] on the CFT side. The interface carries no degrees of freedom in addition to the ones inherited from $\mathcal{N} = 4$ SYM. In this section we will introduce the basic information about the bulk geometries associated to theories with defects, referring in particular to the Janus interface solution.

A. Geometries with defects

An interface CFT with a codimension-one planar defect is invariant under the subgroup $SO(d-1,2)$ of the original conformal group $SO(d,2)$. Its holographic dual is described by AdS_{d+1} space foliated into AdS_d slices with metric [65–68]

$$ds^2 = L^2(A^2(y)ds^2_{AdS_d} + \rho^2(y)dy^2), \tag{2.1}$$

where y is a noncompact coordinate. When $y \to \pm\infty$, we reach the asymptotic regions with the following behavior for the metric coefficients

$$A(y) \to \frac{L_\pm}{2} e^{\pm y \pm c_\pm}, \qquad \rho(y) \to 1. \tag{2.2}$$

In this context, $L_\pm$ and $c_\pm$ are constants which can in principle assume two different values at $y = \pm\infty$. We parametrize the AdS_d slices using Poincaré coordinates

$$ds^2_{AdS_d} = \frac{1}{z^2}(dz^2 - dt^2 + d\vec{x}^2_{d-2}), \tag{2.3}$$

where (t, z) are the time and radial coordinates on each slice and $\vec{x}$ identifies the other orthogonal spatial directions.

Geometries of the kind described by Eq. (2.1) admit a Fefferman-Graham (FG) expansion close to the asymptotically AdS_{d+1} region of spacetime which brings the metric into the form

$$ds^2 = \frac{L^2}{\xi^2}[d\xi^2 + f_1(\xi/\eta)(-dt^2 + d\vec{x}^2) + f_2(\xi/\eta)d\eta^2]. \tag{2.4}$$

Here, ξ is a radial coordinate for the asymptotic AdS_{d+1} metric in Poincaré coordinates, η is boundary direction orthogonal to the interface and f_1, f_2 are two functions encoding the change of coordinates.

Empty AdS_{d+1} space itself can be described in terms of an AdS_d slicing once we identify $A(y) = \cosh y$ and $\rho(y) = 1$ in Eq. (2.1). In this case, the FG expansion brings the metric into the exact Poincaré form

$$ds^2 = \frac{L^2}{\xi^2}(d\xi^2 + d\eta^2 + d\vec{x}^2 - dt^2), \tag{2.5}$$

and the coordinate transformation reads

$$\eta = z\tanh y, \qquad \xi = \frac{z}{\cosh y}. \tag{2.6}$$

In the general case of a defect geometry, it may not be possible to find a closed form for the FG coordinate transformation, but an asymptotic expansion around the Poincaré solution can always be performed [67,69]. The FG expansion of the metric gives a natural prescription to regularize divergent quantities in the bulk geometry, as we will describe in Sec. III A.

B. Nonsupersymmetric Janus AdS_5 geometry

The non-SUSY five-dimensional Janus solution [63,67] is a one-parameter deformation of AdS_5 described in terms of the metric

$$ds^2 = L^2[(\gamma)^{-1}h^2(w)dw^2 + h(w)ds^2_{AdS_4}], \tag{2.7}$$

where γ is the deformation parameter, with range $3/4 \le \gamma \le 1$, and the four-dimensional AdS slice is written in Poincaré coordinates according to Eq. (2.3). The warp factor $h(w)$ is defined as [63,67]

$$h(w) = \gamma\left(1 + \frac{4\gamma - 3}{\wp(w) + 1 - 2\gamma}\right) = \gamma\left(1 + \frac{4\gamma - 3}{\wp(w) - \wp(w_0)}\right), \tag{2.8}$$

where $\wp(w)$ is the Weierstrass elliptic $\wp$-function.[3] The elliptic invariants (g_2, g_3) of the Weierstrass $\wp$-function are

[2]Since the Janus solution breaks all the supersymmetries, the global SO(6) symmetry is no longer an R-symmetry.

[3]We refer the reader to Appendix for more details on the Weierstrass elliptic function.

$$g_2 = 16\gamma(1-\gamma), \qquad g_3 = 4(\gamma-1), \tag{2.9}$$

and w_0 is defined as the positive solution of

$$\wp(w_0) = 2\gamma - 1. \tag{2.10}$$

The spatially varying dilaton of the non-SUSY Janus solution is

$$\phi(w) = \phi_0 + \sqrt{6(1-\gamma)}\left(w + \frac{4\gamma-3}{\wp'(w)} \times \left(\ln\frac{\sigma(w+w_1)}{\sigma(w-w_1)} - 2\zeta(w_1)w\right)\right), \tag{2.11}$$

where σ and ζ denote the Weierstrass functions defined in Eq. (A3) of Appendix, ϕ_0 is a real constant and w_1 is defined by the equation

$$\wp(w_1) = 2(1-\gamma). \tag{2.12}$$

When $\gamma = 1$, the solution reduces to AdS_5 with constant dilaton $\phi = \phi_0$, while $\gamma = 3/4$ leads to a linear dilaton.

The Janus solution is defined in the interval $-w_0 < w < w_0$ since the function $h(w)$, introduced in Eq. (2.8), has simple poles at $w = \pm w_0$. As $w \to \pm w_0$, the Janus deformation asymptotes to AdS_5 with constant dilaton $\phi_\pm = \phi(\pm w_0)$, where $\phi_+ \neq \phi_-$ unless $\gamma = 1$. In other words, for generic γ the Janus solution has two asymptotically AdS_5 regions in which the dilaton takes two different values.

The conformal structure of the Janus AdS_5 geometry is easily determined by means of the change of variables

$$d\mu = \sqrt{\frac{h(w)}{\gamma}}dw, \tag{2.13}$$

which brings the metric into the form

$$ds^2 = L^2 h(\mu)(d\mu^2 + ds^2_{AdS_4}). \tag{2.14}$$

Up to a conformal factor, the boundary metric is four-dimensional Minkowski spacetime. The conformal diagram corresponding to this geometry is shown in Fig. 1.

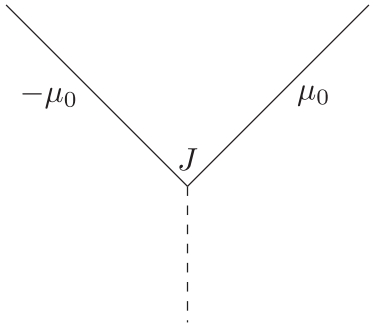

FIG. 1. Conformal diagram of the Janus AdS_5 geometry with Poincaré coordinates on the AdS_4 slices. The angular coordinate is ranged in the interval $[-\mu_0, \mu_0]$, where $\mu_0 > \pi/2$. The dashed line represents the hypersurface $\mu = 0$ intersecting the boundary at the joint J, which is the origin of the angular coordinate. This can be seen as an interface on the boundary. In the diagram we suppress a factor of $\mathbb{R}^2$ at each point.

III. VOLUME FOR THE JANUS AdS_5 GEOMETRY

In this section we study the holographic complexity according to the CV conjecture in the non-SUSY Janus deformed AdS_5 space. In the three-dimensional case, the extremal volume of the entire space for both the Janus AdS_3 [58] and the Randall-Sundrum [54] defect models exhibit a logarithmic divergence. In [56] it is pointed out that, for a boundary CFT (BCFT), the behavior of the divergent terms for the CV conjecture depends on the dimensionality of the space. Since a BCFT can be related to a CFT with a codimension-one defect via the unfolding trick [70], we expect an analogous behavior also for the Janus interface.

A. UV regularizations of the extremal volume

A common feature of geometrical objects defined via the AdS/CFT correspondence is the existence of UV divergences that need to be regularized to describe physically meaningful quantities. This happens, e.g., for the computation of the entanglement entropy, the extremal volume identified by the CV conjecture, or the on-shell gravitational action which plays a role in the computation of free energy or the CA conjecture. There exist essentially three regularization techniques that allow to extract the same physical information [68]. Here, we review the main aspects of these methods.

The extremal volumes that we will compute in this section are of the form

$$\mathcal{V} = \int dz \int dy \int d\vec{x}\,\sqrt{g}, \tag{3.1}$$

where g is the determinant of the induced metric on the codimension-one Cauchy spatial slice. The integrations along the $\vec{x}$ directions are always trivial, while the relevant information on the interface are encoded by the (y, z) directions.

1. Fefferman-Graham regularization

A natural way to regularize UV divergences is provided by the FG metric (2.4). It consists of cutting the geometrical object of interest with the hypersurface located at $\xi = \delta$, and all the results are expressed in terms of a series expansion around $\delta = 0$. The problem of this procedure is that in the region where $\xi/\eta \ll 1$, the FG expansion breaks down and the coordinates (ξ, η) are ill defined [69].

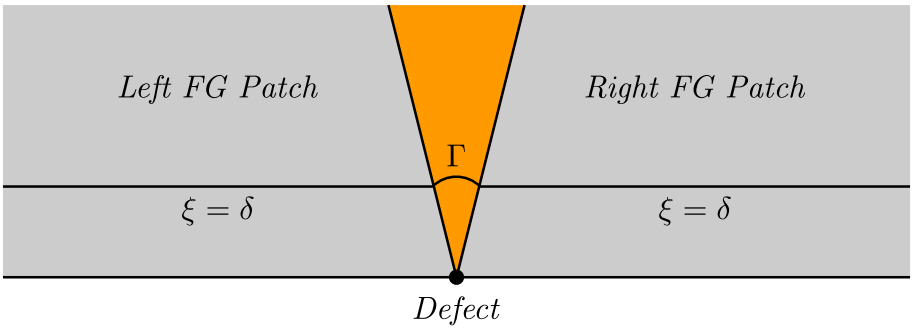

FIG. 2. Interpolation between two FG patches with a continuous curve Γ. The black line, separating the gray region from the orange one (where the FG coordinates are ill defined), corresponds to the value y_0 for the y-coordinate.

Indeed, the defect geometry contains two FG patches located away from the interface on its left and right sides. In the middle region, there is not a well-defined change of variables that selects a natural UV cutoff. This problem can be solved by interpolating the cutoff surface located at $\xi = \delta$ in the left and right FG patches with an arbitrary curve in the middle region, with the constraint that it has to be smooth at $y = y_0$, which corresponds to the breaking down of the FG expansion [54,67]. This setting is depicted in Fig. 2.

2. Single cutoff regularization

This method makes use of the FG expansion of the metric to identify a UV cutoff in the asymptotic region. Instead of performing an arbitrary interpolation in the middle region, it induces a minimal value for the z-coordinate.

We explain the details of the procedure starting from the empty AdS case, whose FG expansion is achieved by means of the coordinate transformation (2.6). If we locate the UV cutoff at the surface $\xi = \delta$, we get the condition

$$\delta = \frac{z}{\cosh y}, \tag{3.2}$$

which selects a maximal value of $y = y^*(z)$ in Eq. (3.1). On the other hand, reversing this identity gives a constraint on the minimal value of the z, determined by

$$z_{\min} = \delta \min_{y\in\mathbb{R}}(\cosh y) = \delta. \tag{3.3}$$

In the presence of an interface, the procedure is formally the same, but the conditions to impose become

$$\delta = \frac{z}{A(y)}, \qquad z_{\min} = \delta \min_{y\in\mathbb{R}}[A(y)], \tag{3.4}$$

where $A(y)$ was introduced in Eq. (2.1). This choice degenerates to the empty AdS case once the deformation parameter of the Janus geometry is turned off. At the end of the procedure, we will perform a Laurent expansion of the result in powers of δ.

We point out that the two regularizations presented (FG expansion and single cutoff) are *a priori* different the FG procedure requires an arbitrary interpolation in the middle region, while the single cutoff uses the FG expansion of the metric as a tool to induce a minimal value for the integration along the z coordinate. However, a careful analysis of the details of the procedure shows that a proper choice of the interpolating curve allows to find the same results up to finite terms, as it was discussed for the three-dimensional case in [58].

3. Double cutoff regularization

Another way to regularize an integration along the two directions (y, z) is to introduce two separate UV cutoffs. A natural choice is to impose $z = \delta$ on the AdS_d slicing instead of making use of the FG expansion. Since the metric factor $A(y)$ is singular at infinity even after this regularization, a maximum value of y is determined by requiring

$$A(y) = \frac{1}{\varepsilon}, \tag{3.5}$$

which is a natural counterpart of Eq. (3.4). Notice that while the δ cutoff has physical relevance as it regularizes the intrinsic contribution from the defect to the volume, the ε cutoff is a mathematical artifact introduced at intermediate steps. This parameter is sent to zero at the end of the computation, and the physical quantities will not depend on it.

B. Extremal volume: single cutoff procedure

We evaluate the extremal volume using the metric in Eq. (2.7). Since the integral that defines the volume diverges near the asymptotic boundary, i.e., when $w \to \pm w_0$ and $z \to 0$, we have to regularize it introducing suitable cutoffs. We adopt the single cutoff regularization procedure

described in Sec. III A, which relies on the intertwining between the UV cutoff along the w and z directions.

1. Determination of the geometric data

First of all, we need to rewrite the metric of Janus AdS_5 space into the general form given in Eq. (2.1), where the coordinate y is noncompact and the prefactor of the dy^2 terms is the unity. This can be easily achieved by performing the following change of coordinates

$$dy = \gamma^{-1/2} h(w) dw \Rightarrow y = \gamma^{-1/2} \int_0^w dw' h(w'), \quad (3.6)$$

which brings the metric (2.7) into the form

$$ds^2 = L^2 (dy^2 + h(y) ds^2_{AdS_4}), \quad (3.7)$$

where we identify

$$A(y) = \sqrt{h(y)}, \qquad \rho(y) = 1. \quad (3.8)$$

According to Eq. (3.4), the cutoff surface at $\xi = \delta$ gives the constraint

$$\delta = \frac{z}{\sqrt{h(y)}}, \quad (3.9)$$

which consequently induces the value of $z_{\min}$ as

$$z_{\min} = \delta \min_{y \in \mathbb{R}} (\sqrt{h(y)}) = \delta \sqrt{\gamma}, \quad (3.10)$$

where we used that h takes minimum value at $y = 0$, and $h(0) = \gamma$. The previous prescription can be equivalently employed using the compact coordinate w and it defines a cutoff $w_\pm$ such that

$$h(w_\pm) = \frac{z^2}{\delta^2} \Rightarrow w_\pm = h^{-1}\left(\frac{z^2}{\delta^2}\right). \quad (3.11)$$

It regularizes the divergencies stemming from the poles of the function $h(w)$ located at $w = \pm w_0$. The cutoff $w_\pm$ can be expanded in a power series of δ/z, as shown in [67]

$$w_\pm\left(\frac{\delta}{z}\right) = \pm w_0 \mp \sum_{k=1}^{\infty} b_k \frac{\delta^{2k}}{z^{2k}}. \quad (3.12)$$

All the coefficients of the series can be recursively determined order by order by imposing the condition (3.11). The previous expression only contains even powers of δ/z because $h(w)$ is an even function, and the first coefficients of the series are given by

$$b_1 = \frac{\sqrt{\gamma}}{2}, \quad b_2 = \frac{\sqrt{\gamma}}{8}, \quad b_3 = \frac{\sqrt{\gamma}}{16}, \quad b_4 = \frac{5\sqrt{\gamma}}{128}, \quad \ldots \quad (3.13)$$

Whereas the location of the cutoff is fixed via a Taylor expansion, the identity (3.11) is exact and formally resums all the coefficients of the above series.

2. Computation of the volume

It is not restrictive to study the CV conjecture in the deformed AdS_5 background using a time slice at zero boundary time.[4] The extremal volume is computed by the integral

$$\mathcal{V} = \frac{2L^4 V_2}{\sqrt{\gamma}} \int_{\delta\sqrt{\gamma}}^{z_{IR}} \frac{dz}{z^3} \int_0^{w_+(\frac{\delta}{z})} h(w)^{\frac{5}{2}} dw, \quad (3.14)$$

where we introduced a factor of two because $\wp(w)$ is even, and we denoted with V_2 the two-dimensional infinite volume along the orthogonal spatial directions. Since the integral along the z direction is in principle divergent at infinity, we regularize it introducing a cutoff z_{IR}.

To evaluate the extremal volume, we begin with the change of variables $\tau = \frac{h(w)}{\gamma}$. The extremes of integration are fixed by the conditions $h(0) = \gamma$ and $h(w_\pm) = z^2/\delta^2$. Using the properties of the Weierstrass $\wp$-function summarized in Appendix, we get

$$\int_0^{w_+(\varepsilon)} dw h^{5/2}(w) = \frac{\gamma^{5/2}}{2} \int_1^{\frac{z^2}{\gamma\delta^2}} d\tau \sqrt{\frac{\tau^5}{\gamma(\tau^4 - 1) - (\tau^3 - 1)}}. \quad (3.15)$$

At this point, we perform a further change of variables $\zeta = z^2/(\gamma\delta^2)$, which brings the volume (3.14) into the form

$$\mathcal{V} = \frac{\gamma L^4 V_2}{2\delta^2} \int_1^{\zeta_{IR}} \frac{d\zeta}{\zeta^2} \int_1^{\zeta} d\tau \, \tau^{5/2} f(\tau), \quad (3.16)$$

where we define

$$f(\tau) \equiv \frac{1}{\sqrt{\gamma(\tau^4 - 1) - (\tau^3 - 1)}}, \qquad \zeta_{IR} \equiv \frac{z_{IR}^2}{\gamma\delta^2}. \quad (3.17)$$

We can swap the order of integration as shown in Fig. 3 in the following way

$$\int_1^{\zeta_{IR}} d\zeta \int_1^{\zeta} d\tau \, F(\tau, \zeta) \to \int_1^{\zeta_{IR}} d\tau \int_\tau^{\zeta_{IR}} d\zeta \, F(\tau, \zeta), \quad (3.18)$$

[4]It can be shown that the extremal slice at constant time is always a solution of the equations of motion at all times. By translational invariance along the time direction, we choose for convenience to study the case with vanishing boundary time.

for any given integrand function $F(\tau,\zeta)$. The evaluation of the ζ integration is trivial and gives

$$\mathcal{V}=\frac{\gamma L^4 V_2}{2\delta^2}\int_1^{\zeta_{\rm IR}} d\tau\,\tau^{5/2} f(\tau)\left(\frac{1}{\tau}-\frac{1}{\zeta_{\rm IR}}\right). \tag{3.19}$$

The remaining integral is divergent in the limit $\delta\to 0$, i.e., $\zeta_{\rm IR}\to\infty$. However, the function $f(\tau)$ can be series-expanded around infinity, where it is analytic. We can add and subtract the lowest orders of the $f(\tau)$ expansion

$$\begin{aligned}\tau^{5/2} f(\tau)\left(\frac{1}{\tau}-\frac{1}{\zeta_{\rm IR}}\right)&=\tau^{3/2}\left[\left(f(\tau)-\frac{1}{\sqrt{\gamma}\tau^2}-\frac{1}{2\gamma^{3/2}\tau^3}\right)+\frac{1}{\sqrt{\gamma}\tau^2}+\frac{1}{2\gamma^{3/2}\tau^3}\right]\\&\quad-\frac{\tau^{5/2}}{\zeta_{\rm IR}}\left[\left(f(\tau)-\frac{1}{\sqrt{\gamma}\tau^2}-\frac{1}{2\gamma^{3/2}\tau^3}\right)+\frac{1}{\sqrt{\gamma}\tau^2}+\frac{1}{2\gamma^{3/2}\tau^3}\right],\end{aligned} \tag{3.20}$$

in such a way that the terms in the round parenthesis define a renormalized finite integral where the limit $\delta\to 0$ can be performed directly. Hence, we define

$$\mathcal{A}(\gamma)\equiv\int_1^{\infty} d\tau\,\tau^{3/2}\left(f(\tau)-\frac{1}{\sqrt{\gamma}\tau^2}-\frac{1}{2\gamma^{3/2}\tau^3}\right), \tag{3.21}$$

$$\mathcal{B}(\gamma)\equiv\int_1^{\infty} d\tau\,\tau^{5/2}\left(f(\tau)-\frac{1}{\sqrt{\gamma}\tau^2}-\frac{1}{2\gamma^{3/2}\tau^3}\right). \tag{3.22}$$

These functions can be numerically evaluated and are well defined everywhere except near $\gamma=3/4$, which is a singular limit since $w_0\to\infty$.

In the following, we will keep implicit the functions $\mathcal{A}(\gamma)$ and $\mathcal{B}(\gamma)$. The divergences in the extremal volume are encoded by the following remaining terms

$$\begin{aligned}&\int_1^{\zeta_{\rm IR}} d\tau\left(\frac{1}{\sqrt{\gamma\tau}}+\frac{1}{2\gamma^{3/2}\tau^{3/2}}\right)\\&\quad=\frac{1}{\gamma^{3/2}}\left(2\gamma\sqrt{\zeta_{\rm IR}}-\frac{1}{\sqrt{\zeta_{\rm IR}}}+1-2\gamma\right),\end{aligned} \tag{3.23}$$

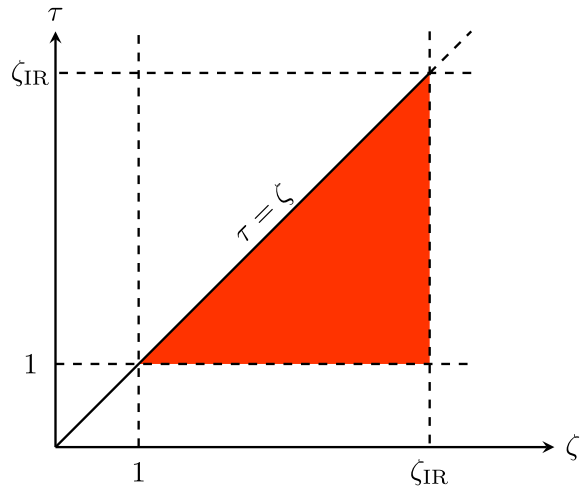

FIG. 3. The domain of integration is depicted in red. We can swap the order of the integrals by adjusting the extremes of integration.

$$\int_1^{\zeta_{\rm IR}} d\tau\left(\sqrt{\frac{\tau}{\gamma}}+\frac{1}{2\gamma^{3/2}\sqrt{\tau}}\right)=\frac{1}{\gamma^{3/2}}\left(\frac{2\gamma}{3}\zeta_{\rm IR}^{3/2}+\sqrt{\zeta_{\rm IR}}-\frac{2}{3}\gamma-1\right). \tag{3.24}$$

Summing all the contributions with the appropriate prefactors, we obtain the expression for the extremal volume,

$$\begin{aligned}\mathcal{V}=L^4V_2\Bigg[&\frac{2}{3}\frac{z_{\rm IR}}{\delta^3}+\left(\frac{\gamma\mathcal{A}(\gamma)}{2}-\sqrt{\gamma}+\frac{1}{2\sqrt{\gamma}}\right)\frac{1}{\delta^2}\\&-\frac{1}{z_{\rm IR}\delta}-\frac{1}{2z_{\rm IR}^2}\left(\gamma^2\mathcal{B}(\gamma)-\sqrt{\gamma}-\frac{2}{3}\gamma^{3/2}\right)\Bigg]+\mathcal{O}(\delta).\end{aligned} \tag{3.25}$$

3. Subtraction of vacuum $\mathbf{AdS_5}$

To identify the contribution of the defect to the extremal volume, we need to subtract the result that stems from vacuum AdS_5. First of all, we write the AdS_5 metric in AdS_4 sliced form by setting $\gamma\to 1$ in Eq. (2.7), recognizing that in this limit

$$h(w)=\frac{1}{1-w^2},\qquad w_0=1. \tag{3.26}$$

Thus, the AdS_5 metric can be rewritten as

$$ds^2_{AdS_5}=\frac{L^2dw^2}{(1-w^2)^2}+\frac{L^2}{1-w^2}ds^2_{AdS_4}. \tag{3.27}$$

Notice that the same result can be achieved by performing the change of coordinates

$$w=\tanh y \tag{3.28}$$

in the standard unit-radius AdS_5 metric written in Poincaré slicing

$$ds^2_{\mathrm{AdS}_5} = dy^2 + \cosh^2 y ds^2_{\mathrm{AdS}_4}. \tag{3.29}$$

The FG change of coordinates (2.6) for the metric (3.27) becomes

$$\xi = z\sqrt{1-w^2}, \qquad \eta = zw, \tag{3.30}$$

and, by setting $\xi = \delta$, they induce a cutoff w_* given by

$$w_* = \sqrt{1-\frac{\delta^2}{z^2}}. \tag{3.31}$$

The value of $z_{\min}$ is defined as

$$z_{\min} = \min\left(\frac{\delta}{\sqrt{1-w^2}}\right) = \delta. \tag{3.32}$$

The extremal volume at $t=0$ for the AdS_5 vacuum solution reads

$$\begin{aligned}\mathcal{V}_{\mathrm{AdS}_5} &= 2L^4V_2\int_\delta^{z_{\mathrm{IR}}}\frac{dz}{z^3}\int_0^{\sqrt{1-\frac{\delta^2}{z^2}}}\frac{dw}{(1-w^2)^{5/2}} \\ &= 2L^4V_2\left[\frac{1}{3}\frac{z_{\mathrm{IR}}}{\delta^3}-\frac{1}{2}\frac{1}{z_{\mathrm{IR}}\delta}\right]+\mathcal{O}(\delta).\end{aligned} \tag{3.33}$$

4. Total result

Once we subtract the volume for the empty AdS_5 space to Eq. (3.25), we obtain the complexity of formation of the Janus AdS_5 solution as

$$\begin{aligned}\Delta\mathcal{C}_{\mathrm{AdS}_5}(\gamma) = &\frac{V_2L^3}{G\delta^2}\left(\frac{\gamma\mathcal{A}(\gamma)}{2}-\sqrt{\gamma}+\frac{1}{2\sqrt{\gamma}}\right) \\ &-\frac{V_2L^3}{2Gz_{\mathrm{IR}}^2}\left(\gamma^2\mathcal{B}(\gamma)-\sqrt{\gamma}-\frac{2}{3}\gamma^{3/2}\right)+\mathcal{O}(\delta).\end{aligned} \tag{3.34}$$

This result shows that the contribution to the complexity intrinsic to the interface amounts to a power-law divergence δ^{-2} and to a finite part, which vanishes in the limit $z_{\mathrm{IR}}\to\infty$. We will comment on this structure with further details after having studied the complexity of formation with the double cutoff regularization scheme.

C. Extremal volume: Double cutoff procedure

We employ the double cutoff prescription to regularize the UV divergences of the extremal volume. Since we introduce two different regulators for the z and w directions, the integrations are not nested. We select the UV cutoff along the z direction to be $z=\delta$, whereas to determine a cutoff in the w variable we use

$$h(w_\pm) = \frac{1}{\varepsilon^2}, \tag{3.35}$$

according to Eq. (3.5).

1. Computation of the volume

The extremal volume at vanishing boundary time is determined by

$$\mathcal{V} = \frac{2L^4V_2}{\sqrt{\gamma}}\int_\delta^{z_{\mathrm{IR}}}\frac{dz}{z^3}\int_0^{w_+(\varepsilon)}h(w)^{\frac{5}{2}}dw. \tag{3.36}$$

Changing variables into $\tau = h(w)/\gamma$ and performing the integration over z, we obtain

$$\mathcal{V} = \frac{\gamma^2L^4V_2}{2\delta^2}\left(\frac{1}{2\delta^2}-\frac{1}{2z_{\mathrm{IR}}^2}\right)\int_1^{\frac{1}{\gamma\varepsilon^2}}d\tau\tau^{5/2}f(\tau). \tag{3.37}$$

The last integration in τ is carried out using the same method described in Sec. III B. Thus, the extremal volume in the double cutoff regularization scheme reads

$$\begin{aligned}\mathcal{V} = &\frac{L^4V_2}{2}\left(\frac{1}{\delta^2}-\frac{1}{z_{\mathrm{IR}}^2}\right)\left(\frac{2}{3\varepsilon^3}+\frac{1}{\varepsilon}+\gamma^2\mathcal{B}(\gamma)\right. \\ &\left.-\sqrt{\gamma}-\frac{2}{3}\gamma^{3/2}\right)+\mathcal{O}(\varepsilon).\end{aligned} \tag{3.38}$$

2. Subtraction of vacuum AdS_5

With this other regularization, the cutoff along the w coordinate is determined as

$$h(w^*) = \frac{1}{1-(w^*)^2} = \frac{1}{\varepsilon^2} \quad\Rightarrow\quad w^* = \sqrt{1-\varepsilon^2}. \tag{3.39}$$

Thus, the extremal volume for the undeformed case is

$$\begin{aligned}\mathcal{V}_{\mathrm{AdS}_5} &= 2L^4V_2\int_\delta^\infty\frac{dz}{z^3}\int_0^{\sqrt{1-\varepsilon^2}}\frac{dw}{(1-w^2)^{5/2}} \\ &= \frac{L^4V_2}{\delta^2}\left(\frac{1}{3\varepsilon^3}+\frac{1}{2\varepsilon}\right)+\mathcal{O}(\varepsilon).\end{aligned} \tag{3.40}$$

3. Total result

After subtracting the vacuum solution from the extremal volume (3.38) in the presence of the defect, we get the complexity of formation

$$\Delta\mathcal{C}_{\mathrm{AdS}_5} = \frac{V_2L^3}{2G}\left(\gamma^2\mathcal{B}(\gamma)-\sqrt{\gamma}-\frac{2}{3}\gamma^{3/2}\right)\left(\frac{1}{\delta^2}-\frac{1}{z_{\mathrm{IR}}^2}\right). \tag{3.41}$$

Comparing this result with Eq. (3.34), we notice that the coefficient of the divergent part is different, while the finite

terms match. This suggests that the universal information encoded by the complexity of formation is associated to the finite part, since a change of the energy scale does not affect it. We should also emphasize that the finite part is inversely proportional to the IR regulator, and then in the smooth limit $z_{\mathrm{IR}} \to \infty$ the corresponding expression vanishes. Therefore, no universal information is encoded in the complexity of formation for the entire Janus AdS_5 geometry, except that divergences scale as δ^{-2}.

IV. VOLUME SUBREGION FOR THE JANUS AdS_5 GEOMETRY

In this section we move to the case of subregion complexity to analyze if additional divergences (e.g., logarithms in the UV cutoff) arise in the computation of the extremal volume. If further types of divergences occur, we can get additional insights into the structure of universal terms in the complexity of formation.

In the CV case, subregion complexity is computed as the volume of a maximal codimension-one bulk surface enclosed by the boundary subregion and the corresponding Hubeny-Rangamani-Takayanagi surface [71]. In the CA case, it is computed as the gravitational action in the intersection region between the WDW patch and the entanglement wedge built from the boundary subregion [32]. Subregion complexity has been investigated for asymptotically AdS_3 spacetime, where it was found that the volume depends only on topological quantities but not on the temperature of the black hole [72]. Contrarily, the action for a generic segment on the boundary of the Banados-Teitelboim-Zanelli (BTZ) black hole is not topological, but is directly related to the corresponding entanglement entropy. This structure is spoiled when a larger number of intervals on the boundary is considered [73]. From the field theory point of view, subregion complexity is believed to be dual either to fidelity, complexity of purification, or basis complexity [71,74,75].

A. Ball-shaped subregion on the boundary

Following ideas similar to the ones used to investigate entanglement entropy in [67,68], a particularly convenient scenario in which to study the subregion complexity, corresponds to a ball-shaped region of radius R centered on the interface, see Fig. 4. It is possible to show that the RT surface corresponding to such subsystem reads

$$z^2 + r^2 = R^2, \tag{4.1}$$

where this equation is written in terms of the metric (2.7) with the two-dimensional subspace parametrized with polar coordinates

$$d\vec{x}^2 = dr^2 + r^2 d\theta^2. \tag{4.2}$$

Remarkably, the spacelike RT surface in Eq. (4.1) is the same found in empty AdS_5 space. In fact, it can be shown that it also corresponds to a global minimum of the area functional in the Janus AdS_5 geometry.

The RT surface delimits the region where the extremal codimension-one Cauchy slice, that computes the extremal volume, extends. Thus, the integration domain of the volume will be modified and will not reach $z = z_{\mathrm{IR}}$, as it happens instead in the full Janus AdS_5 case. Now, we need to evaluate

$$\mathcal{V}_{\mathrm{sub}}(R,\gamma) = \frac{2L^4}{\sqrt{\gamma}} \int_0^{2\pi} d\theta \int_{z_{\mathrm{min}}}^{z_{\mathrm{max}}} \frac{dz}{z^3} \int_0^{\sqrt{R^2-z^2}} dr\, r \times \int_0^{w_+} dw\, h^{\frac{5}{2}}(w), \tag{4.3}$$

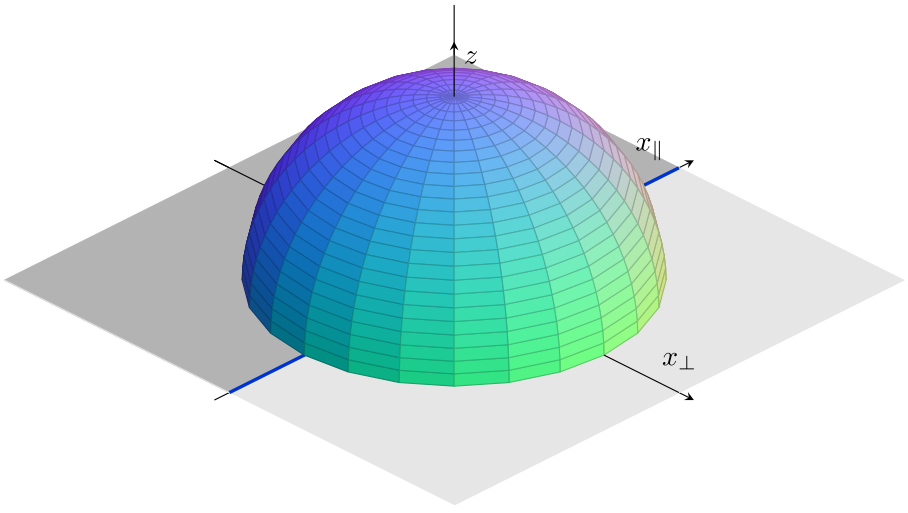

FIG. 4. Time slice of the Janus AdS_5 spacetime with a ball-shaped subregion centered on the interface. The Ryu-Takayanagi surface is represented by the spherical dome while the blue line represents the interface located at $x_\perp = 0$.

where we put a factor of two for symmetry reasons in the w integration. The integral along the angular direction is trivial, while the one along the radial direction of the polar coordinates gives an additional factor that will modify the last integration along z. It is straightforward to find

$$\mathcal{V}_{\rm sub}(R,\gamma)=\frac{2\pi L^4}{\sqrt{\gamma}}\int_{z_{\rm min}}^{R}dz\frac{R^2-z^2}{z^3}\int_0^{w_+}dw\,h^{\frac{5}{2}}(w). \tag{4.4}$$

Notice that the maximum value that can be reached by z is R. Otherwise, the square root defining the maximum of the radial coordinate r would be imaginary. The minimum of z is determined in the same way as for the total volume, according to Eq. (3.10) for the single cutoff prescription, whereas for the double cutoff regularization corresponds to $z_{\rm min}=\delta$.

B. Extremal volume: Single cutoff procedure

We start by computing the extremal volume for the ball-shaped region in the Janus AdS_5 geometry using the single cutoff method. Once more it is useful to change variables in

$$\tau=\frac{h(w)}{\gamma},\qquad \zeta=\frac{z^2}{\gamma\delta^2}, \tag{4.5}$$

so that the integral in Eq. (4.4) becomes

$$\mathcal{V}_{\rm sub}(R,\gamma)=\pi L^4\gamma^2\int_1^{\frac{R^2}{\gamma\delta^2}}d\zeta\frac{R^2-\gamma\delta^2\zeta}{2\gamma\delta^2\zeta^2}\int_1^{\zeta}d\tau\,\tau^{5/2}f(\tau). \tag{4.6}$$

As explained in Eq. (3.18) for the total Janus AdS_5 space, we can swap the integrals in ζ and τ being mindful to perform the suitable changes in the extremes of integration, getting

$$\mathcal{V}_{\rm sub}(R,\gamma)=\pi L^4\gamma^2\int_1^{\frac{R^2}{\gamma\delta^2}}d\tau\,\tau^{5/2}f(\tau)\int_\tau^{\frac{R^2}{\gamma\delta^2}}d\zeta\frac{R^2-\gamma\delta^2\zeta}{2\gamma\delta^2\zeta^2}. \tag{4.7}$$

Now, it is possible to evaluate first the integral in the ζ variable as

$$\int_\tau^{\frac{R^2}{\gamma\delta^2}}d\zeta\frac{R^2-\gamma\delta^2\zeta}{2\gamma\delta^2\zeta^2}=\frac{1}{2}\left(2\log\left(\frac{\sqrt{\gamma}\delta}{R}\right)-1+\frac{R^2}{\gamma\delta^2\tau}+\log\tau\right). \tag{4.8}$$

Concerning the integration over τ, we have to compute three different kinds of integrals. The first one can be evaluated following the same steps as in Sec. III B

$$\begin{aligned}\int_1^{\frac{R^2}{\gamma\delta^2}}d\tau\,\tau^{5/2}f(\tau)&=\mathcal{B}(\gamma)+\int_1^{\frac{R^2}{\gamma\delta^2}}\left(\sqrt{\frac{\tau}{\gamma}}+\frac{1}{2\gamma^{3/2}\sqrt{\tau}}\right)\\&=\mathcal{B}(\gamma)+\frac{2R^3}{3\gamma^2\delta^3}+\frac{R}{2\gamma\delta^2}-\frac{1}{\gamma^{3/2}}-\frac{2}{3\sqrt{\gamma}},\end{aligned} \tag{4.9}$$

where $\mathcal{B}(\gamma)$ is defined in Eq. (3.22) and we have taken the $\delta\to 0$ limit.

The second integral in τ is given by

$$\begin{aligned}\int_1^{\frac{R^2}{\gamma\delta^2}}d\tau\,\tau^{3/2}f(\tau)&=\mathcal{A}(\gamma)+\int_1^{\frac{R^2}{\gamma\delta^2}}\left(\frac{1}{\sqrt{\gamma\tau}}+\frac{1}{2\gamma^{3/2}\tau^{3/2}}\right)\\&=\mathcal{A}(\gamma)+\frac{2R}{\gamma\delta}+\frac{1}{\gamma^{3/2}}-\frac{2}{\sqrt{\gamma}}-\frac{\delta}{\gamma R}.\end{aligned} \tag{4.10}$$

Here, $\mathcal{A}(\gamma)$ is defined as in Eq. (3.21). Since the result of the integral has to be multiplied by a factor of $R^2/(\gamma\delta^2)$ coming from the ζ integration, it is crucial to expand the above expression up to order δ to keep track of all the possible divergences.

The last type of integral in τ is

$$\begin{aligned}&\int_1^{\frac{R^2}{\gamma\delta^2}}d\tau\,\tau^{5/2}\log\tau\,f(\tau)\\&=C(\gamma)+\int_1^{\frac{R^2}{\gamma\delta^2}}\left(\frac{\log\tau\sqrt{\tau}}{\sqrt{\gamma}}+\frac{\log\tau}{2\gamma^{3/2}\sqrt{\tau}}\right)\\&=C(\gamma)-\log\left(\frac{\sqrt{\gamma}\delta}{R}\right)\left(\frac{4R^3}{3\gamma^2\delta^3}+\frac{2R}{\gamma^2\delta}\right)\\&\quad-\frac{4R^3}{9\gamma^2\delta^3}-\frac{2R}{\gamma^2\delta}+\frac{2}{\gamma^{3/2}}+\frac{4}{9\sqrt{\gamma}},\end{aligned} \tag{4.11}$$

where we define

$$C(\gamma)=\int_1^{\infty}d\tau\,\tau^{5/2}\log\tau\left(f(\tau)-\frac{1}{\sqrt{\gamma}\tau^2}-\frac{1}{2\gamma^{3/2}\tau^3}\right). \tag{4.12}$$

This function can be evaluated numerically and it is analytic in all the range $3/4\le\gamma\le 1$. Nevertheless, we will keep it implicit in the following manipulations.

Combining together all the terms, we get the extremal subregion volume

$$\begin{aligned}\mathcal{V}_{\rm sub}(R,\gamma)&=\frac{4\pi L^4}{9}\frac{R^3}{\delta^3}+\pi L^4\frac{R^2}{\delta^2}\left(\frac{\gamma\mathcal{A}(\gamma)}{2}-\sqrt{\gamma}+\frac{1}{2\sqrt{\gamma}}\right)-2\pi L^4\frac{R}{\delta}\\&\quad+\pi L^4\log\left(\frac{\sqrt{\gamma}\delta}{R}\right)\left(\gamma^2\mathcal{B}(\gamma)-\sqrt{\gamma}-\frac{2}{3}\gamma^{3/2}\right)+\frac{\pi L^4}{2}\left(\gamma^2C(\gamma)-\gamma^2\mathcal{B}(\gamma)+3\sqrt{\gamma}+\frac{10}{9}\gamma^{3/2}\right).\end{aligned} \tag{4.13}$$

1. Subtraction of the vacuum AdS solution

Now, we can perform the subtraction of the AdS vacuum solution, which corresponds to set $\gamma = w_0 = 1$. The volume reads

$$\mathcal{V}_{\rm sub}(R,\gamma=1) = 2\pi L^4 \int_\delta^R dz \frac{R^2-z^2}{z^3} \int_0^{\sqrt{1-\frac{\delta^2}{z^2}}} \frac{dw}{(1-w^2)^{\frac{5}{2}}} = \frac{4\pi L^4}{9}\frac{R^3}{\delta^3} - 2\pi L^4 \frac{R}{\delta} + \frac{2\pi^2 L^4}{3} + \mathcal{O}(\delta). \tag{4.14}$$

2. Total result

Subtracting the undeformed AdS_5 solution to the extremal volume obtained in Eq. (4.13), we find that the subregion complexity of formation is given by

$$\Delta\mathcal{C}_{\rm sub}(R,\gamma) = \frac{\pi L^3 R^2}{G\ \delta^2}\left(\frac{\gamma\mathcal{A}(\gamma)}{2} - \sqrt{\gamma} + \frac{1}{2\sqrt{\gamma}}\right) + \frac{\pi L^3}{G}\log\left(\frac{\sqrt{\gamma}\delta}{R}\right)\left(\gamma^2\mathcal{B}(\gamma) - \sqrt{\gamma} - \frac{2}{3}\gamma^{3/2}\right) + \frac{\pi L^3}{2G}\left(\gamma^2 C(\gamma) - \gamma^2\mathcal{B}(\gamma) + 3\sqrt{\gamma} + \frac{10}{9}\gamma^{3/2} - \frac{4\pi}{3}\right). \tag{4.15}$$

A comment on the limit $R \to \infty$ is in order. This limit corresponds to the case where the subregion covers the entire boundary, and should therefore map to the result for the total volume computed in Eq. (3.34). In order to verify that this is the case, we notice that in polar coordinates the two-dimensional volume along the spatial directions $\vec{x} = (r,\theta)$ is

$$V_2 = \pi R^2, \tag{4.16}$$

which becomes infinite in the limit $R \to \infty$. For this reason, when comparing the two quantities we should check that

$$\frac{\Delta\mathcal{V}}{V_2} = \lim_{R\to\infty}\frac{\Delta\mathcal{V}_{\rm sub}}{\pi R^2}. \tag{4.17}$$

The limit in the rhs of Eq. (4.17) suppresses logarithmic and finite terms, and allows us only to compare the divergent parts which are proportional to the volume of the subregion. Employing Eq. (4.17), we immediately recognize that the terms proportional to δ^{-2} in Eqs. (3.34) and (4.15) exactly match. In conclusion, the difference between the total and the subregion case for the complexity = volume conjecture involving the Janus deformation of AdS_5 spacetime, amounts to the presence of an additional finite term and a logarithmic divergence.

C. Extremal volume: Double cutoff procedure

We evaluate the volume in Eq. (4.4) using the double cutoff regularization scheme, which consists in setting $z_{\rm min} = \delta$. The integral along the z variable reads

$$\int_\delta^R dz \frac{R^2-z^2}{z^3} = \frac{R^2}{2\delta^2} + \log\left(\frac{\delta}{R}\right) - \frac{1}{2}. \tag{4.18}$$

After the change of variables $\tau = \gamma^{-1}h(w)$, the volume becomes

$$\mathcal{V}_{\rm sub}(R,\gamma) = \pi L^4\gamma^2\left(\frac{R^2}{2\delta^2} + \log\left(\frac{\delta}{R}\right) - \frac{1}{2}\right)\int_1^{\frac{1}{\gamma\varepsilon^2}} d\tau\,\tau^{5/2} f(\tau) = \pi L^4\left(\frac{R^2}{2\delta^2} + \log\left(\frac{\delta}{R}\right) - \frac{1}{2}\right) \times \left(\gamma^2\mathcal{B}(\gamma) + \frac{2}{3\varepsilon^3} + \frac{1}{\varepsilon} - \sqrt{\gamma} - \frac{2}{3}\gamma^{3/2}\right) + \mathcal{O}(\varepsilon). \tag{4.19}$$

1. Subtraction of the vacuum AdS solution

The corresponding volume in the empty AdS geometry is easily obtained by considering

$$\mathcal{V}_{\rm sub}(R,0) = 2\pi L^4 \int_\delta^R dz \frac{R^2-z^2}{z^3}\int_0^{\sqrt{1-\varepsilon^2}} \frac{dw}{(1-w^2)^{5/2}} = 2\pi L^4\left(\frac{R^2}{2\delta^2} + \log\left(\frac{\delta}{R}\right) - \frac{1}{2}\right)\left(\frac{1}{3\varepsilon^3} + \frac{1}{2\varepsilon}\right) + \mathcal{O}(\varepsilon). \tag{4.20}$$

2. Total result

After subtracting the vacuum solution from Eq. (4.19), we get the complexity of formation in the double cutoff regularization scheme

$$\Delta\mathcal{C}_{\rm sub}(R,\gamma) = \frac{\pi L^3}{G}\left(\frac{R^2}{2\delta^2} + \log\left(\frac{\delta}{R}\right) - \frac{1}{2}\right) \times \left(\gamma^2\mathcal{B}(\gamma) - \sqrt{\gamma} - \frac{2}{3}\gamma^{3/2}\right) + \mathcal{O}(\varepsilon). \tag{4.21}$$

It can be easily checked that in the $R \to \infty$ limit, one finds

$$\lim_{R\to\infty}\frac{V_2 L^4}{\pi R^2}\Delta\mathcal{C}_{\rm sub}(R,\gamma) = \frac{V_2}{2G\delta^2}\left(\gamma^2\mathcal{B}(\gamma) - \sqrt{\gamma} - \frac{2}{3}\gamma^{3/2}\right), \tag{4.22}$$

which matches the δ^{-2} divergent part in Eq. (3.41).

TABLE I. Coefficients of the divergences entering the complexity of formation for the non-SUSY Janus AdS_5 geometry. They can be read from Eqs. (3.34), (3.41), (4.15), and (4.21).

Complexity of formation	Single cutoff	Double cutoff
Entire boundary	$\frac{L^3}{G}\frac{V_2}{\delta^2}\mathcal{F}(\gamma)$	$\frac{L^3}{G}\frac{V_2}{\delta^2}\mathcal{G}(\gamma)$
Subregion: δ^{-2} term	$\frac{L^3}{G}\frac{\pi R^2}{\delta^2}\mathcal{F}(\gamma)$	$\frac{L^3}{G}\frac{\pi R^2}{\delta^2}\mathcal{G}(\gamma)$
Subregion: $\log\delta$ term	$\frac{2\pi L^3}{G}\log(\frac{\delta}{R})\mathcal{G}(\gamma)$	$\frac{2\pi L^3}{G}\log(\frac{\delta}{R})\mathcal{G}(\gamma)$

V. CONCLUSIONS

We computed the holographic complexity of formation for the Janus deformation of AdS_5 spacetime with respect to vacuum space both for the entire boundary and for the case of a symmetric ball-shaped subregion located symmetrically around the interface. We employed two different prescriptions to regularize the extremal volume, i.e., the single and double cutoff methods. The coefficients of the UV divergences are collected in Table I, expressed in terms of the following functions

$$\mathcal{F}(\gamma)\equiv\frac{\gamma\mathcal{A}(\gamma)}{2}-\sqrt{\gamma}+\frac{1}{2\sqrt{\gamma}},\quad \mathcal{G}(\gamma)\equiv\frac{\gamma^2\mathcal{B}(\gamma)}{2}-\frac{\sqrt{\gamma}}{2}-\frac{1}{3}\gamma^{3/2}. \tag{5.1}$$

These functions are depicted in Fig. 5, while the functions $\mathcal{A}(\gamma)$, $\mathcal{B}(\gamma)$ were defined in Eqs. (3.21) and (3.22).

First of all, we notice that the structure of divergences differs between the entire boundary case and the subregion setting. The former is characterized by a power-law divergence δ^{-2}, which is consistent with the result computed in [56] for a BCFT. The subregion complexity, on the other hand, has a richer structure, where an additional logarithmic divergence and a nonvanishing finite terms appears. A similar difference is also present in the complexity = action computation involving the $(2+1)$-dimensional vacuum AdS or BTZ black hole solutions [73].

Comparing the entries in Table I, the only result independent of the regularization scheme is the coefficient of the logarithmic divergences in the subregion case.[5] In addition, the finite term in the total volume case also matches between single and double cutoff prescriptions, see Eqs. (3.34) and (3.41), but it vanishes once we take the limit $z_{\mathrm{IR}}\to\infty$ for the IR regulator. This behavior suggests that similarly to the entanglement entropy computation, universal properties about complexity are encoded by logarithmic or finite terms since they are invariant under rescalings of the UV cutoff. When both terms are present, only the coefficient of the logarithm is universal. In fact, a transformation of the UV cutoff in the logarithm amounts to an additional finite part, which then becomes ambiguous.

[5]Notice that the results for the logarithmic terms in Eqs. (4.15) and (4.21) only differ by $\frac{\pi L^3}{G}\log\gamma$, which however is a finite part.

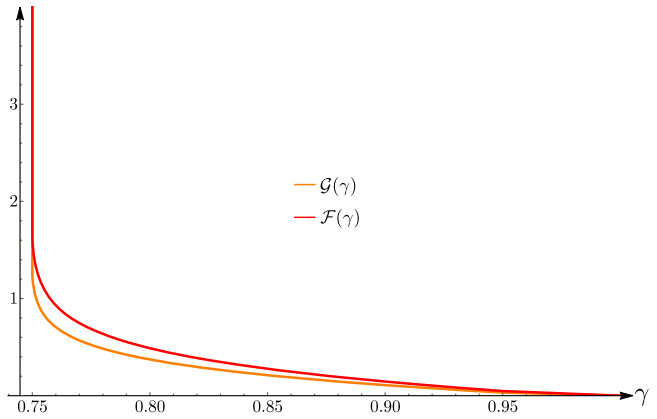

FIG. 5. Numerical plot of the functions $\mathcal{F}(\gamma)$ and $\mathcal{G}(\gamma)$ defined in Eq. (5.1). Both functions vanish in the limit $\gamma\to 1$.

Such remark is also consistent with the three-dimensional case considered in [58], where the complexity of formation was composed by a logarithmic divergence and a finite term in the Janus AdS_3 and in the static Janus BTZ backgrounds. In both cases, distinct regularizations differ by the finite part, but lead to the same coefficient of the logarithmic divergence.

In relation to the three-dimensional case, it is also interesting to compare the dependence of the universal coefficients of the complexity of formation from the deformation parameter. For convenience, we report the logarithmically divergent part of the complexity of formation [58]

$$\Delta\mathcal{C}^{3\mathrm{d}}_{\mathrm{sub}}(l,\gamma_0)=-\frac{L}{G}\eta(\gamma_0)\log\left(\frac{2\delta}{l}\right)+\text{finite}, \tag{5.2}$$

where the function $\eta(\gamma_0)$ is depicted in Fig. 6. The computation refers to the subregion volume for a segment of length l located symmetrically at the boundary.

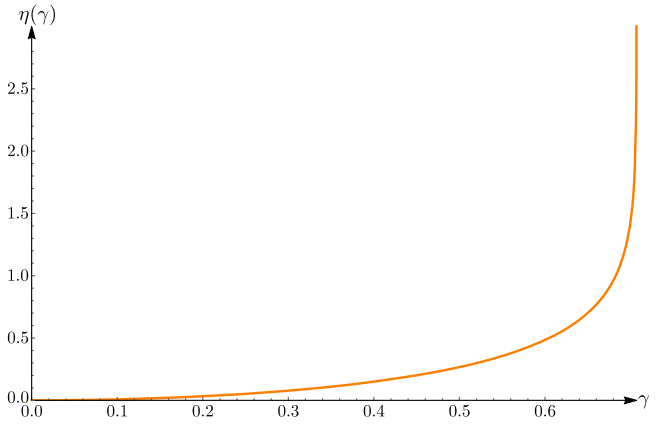

FIG. 6. Plot of $\eta(\gamma)$ as defined in Eq. (5.2), which is the coefficient of the logarithmic divergence due to the defect in the complexity of formation of the Janus AdS_3 geometry.

We compare the function $\eta(\gamma_0)$ describing the universal part of the three-dimensional complexity of formation with the functions $\mathcal{F}(\gamma)$, $\mathcal{G}(\gamma)$ obtained in the five-dimensional case. First of all, it is important to notice that the three-dimensional deformation parameter ranges over $\gamma_0 \in [0, \frac{1}{\sqrt{2}}]$, where $\gamma_0 = 0$ corresponds to empty AdS space (analog to $\gamma = 1$ in five dimensions), and $\gamma_0 = \frac{1}{\sqrt{2}}$ is the maximal deformation (analog to $\gamma = \frac{3}{4}$ in five dimensions). Given this dictionary, we notice that both in three and five dimensions the universal coefficients vanish in the empty AdS case, and diverge when the dilatonic deformation is increased. While the sign of the functions in three and five dimensions is different, we observe that both of them have a monotonic behavior. This could suggest a relation with irreversibility properties of the RG flows similar to the g-theorem for the entanglement entropy, which measures the number of degrees of freedom localized on the defect [76]. We leave the investigation of such properties for future works.

There are some other natural developments of this work that we aim to investigate. A classification of the UV divergences for the complexity = action conjecture in the Janus AdS_5 background would shed more light on the persistency of universality encoded by the logarithmic or finite terms in the volume case. Moreover, this will allow us to compare the UV divergences between the volume and the action cases in a higher-dimensional defect geometry, as was accomplished in [56] for a BCFT. Similarly to their approach, a computation on the field theory side would guide us towards a deeper understanding of the properties of complexity in the presence of an interface. One can perform this investigation using the path integral approach [30], or by studying the geometry that arise in a dual CFT where some of its symmetries are broken, generalizing the method used in [29] to the case of interfaces. The computation for the extremal volume can also be pursued for the higher dimensional generalizations of the time-dependent Janus BTZ black hole proposed in [77].

ACKNOWLEDGMENTS

We thank Roberto Auzzi and Giuseppe Nardelli for many valuable discussions. The authors acknowledge support from the Independent Research Fund Denmark Grant No. DFF-6108-00340 "Towards a deeper understanding of black holes with non-relativistic holography" and from DFF-FNU through Grant No. DFF-4002-00037.

APPENDIX: WEIERSTRASS $\wp$ FUNCTION

The Weierstrass $\wp$ is an elliptic function of order two defined by the series

$$\wp(z,\omega_1,\omega_2) = \frac{1}{z^2} + \sum_{(m,n)\neq(0,0)} \left[\frac{1}{(z-2m\omega_1-2n\omega_2)^2} - \frac{1}{(2m\omega_1+2n\omega_2)^2} \right], \tag{A1}$$

which is doubly periodic in the complex plane with half-periods ω_1, ω_2. It is a meromorphic and even function of z with double poles at the lattice point defined by its periods. One can alternatively define the elliptic $\wp$-function in terms of its invariants g_2, g_3, which can be computed as Eisenstein series involving the half-periods ω_1, ω_2. However, in this case it is simpler to define the $\wp$-function as the solution to the differential equation

$$(\partial_z \wp)^2 = 4\wp^3 - g_2\wp - g_3. \tag{A2}$$

We also define the Weierstrass ζ and σ-functions as

$$\wp(z) = -\zeta'(z), \qquad \zeta(z) = \frac{\sigma'(z)}{\sigma(z)}. \tag{A3}$$

[1] J. M. Maldacena, The large N limit of superconformal field theories and supergravity, Adv. Theor. Math. Phys. **2**, 231 (1998).
[2] S. Ryu and T. Takayanagi, Holographic Derivation of Entanglement Entropy from AdS/CFT, Phys. Rev. Lett. **96**, 181602 (2006).
[3] L. Susskind, Entanglement is not enough, Fortschr. Phys. **64**, 49 (2016).
[4] D. Stanford and L. Susskind, Complexity and shock wave geometries, Phys. Rev. D **90**, 126007 (2014).
[5] A. R. Brown, D. A. Roberts, L. Susskind, B. Swingle, and Y. Zhao, Complexity, action, and black holes, Phys. Rev. D **93**, 086006 (2016).
[6] A. R. Brown, D. A. Roberts, L. Susskind, B. Swingle, and Y. Zhao, Holographic Complexity Equals Bulk Action?, Phys. Rev. Lett. **116**, 191301 (2016).
[7] L. Lehner, R. C. Myers, E. Poisson, and R. D. Sorkin, Gravitational action with null boundaries, Phys. Rev. D **94**, 084046 (2016).

[8] D. Carmi, S. Chapman, H. Marrochio, R. C. Myers, and S. Sugishita, On the time dependence of holographic complexity, J. High Energy Phys. 11 (2017) 188.
[9] S. Chapman, H. Marrochio, and R. C. Myers, Complexity of formation in holography, J. High Energy Phys. 01 (2017) 062.
[10] M. Moosa, Evolution of complexity following a global quench, J. High Energy Phys. 03 (2018) 031.
[11] S. Chapman, H. Marrochio, and R. C. Myers, Holographic complexity in Vaidya spacetimes. Part I, J. High Energy Phys. 06 (2018) 046.
[12] S. Chapman, H. Marrochio, and R. C. Myers, Holographic complexity in Vaidya spacetimes. Part II, J. High Energy Phys. 06 (2018) 114.
[13] J. L. F. Barbon and E. Rabinovici, Holographic complexity and spacetime singularities, J. High Energy Phys. 01 (2016) 084.
[14] M. Alishahiha, A. Faraji Astaneh, M. R. Mohammadi Mozaffar, and A. Mollabashi, Complexity growth with lifshitz scaling and hyperscaling violation, J. High Energy Phys. 07 (2018) 042.
[15] R. Auzzi, S. Baiguera, and G. Nardelli, Volume and complexity for warped AdS black holes, J. High Energy Phys. 06 (2018) 063.
[16] R. Auzzi, S. Baiguera, M. Grassi, G. Nardelli, and N. Zenoni, Complexity and action for warped AdS black holes, J. High Energy Phys. 09 (2018) 013.
[17] M. Alishahiha, A. Faraji Astaneh, A. Naseh, and M. H. Vahidinia, On complexity for F(R) and critical gravity, J. High Energy Phys. 05 (2017) 009.
[18] M. Ghodrati, Complexity growth in massive gravity theories, the effects of chirality, and more, Phys. Rev. D **96**, 106020 (2017).
[19] M. A. Nielsen, M. R. Dowling, M. Gu, and A. C. Doherty, Quantum computation as geometry, Science **311**, 1133 (2006).
[20] M. R. Dowling and M. A. Nielsen, The geometry of quantum computation, Quantum Inf. Comput. **8**, 861 (2008).
[21] R. Auzzi, S. Baiguera, G. B. De Luca, A. Legramandi, G. Nardelli, and N. Zenoni, Geometry of quantum complexity, Phys. Rev. D **103**, 106021 (2021).
[22] V. Balasubramanian, M. Decross, A. Kar, and O. Parrikar, Quantum complexity of time evolution with chaotic Hamiltonians, J. High Energy Phys. 01 (2020) 134.
[23] V. Balasubramanian, M. Decross, A. Kar, C. Li, and O. Parrikar, Complexity growth in integrable and chaotic models, J. High Energy Phys. 07 (2021) 011.
[24] R. Jefferson and R. C. Myers, Circuit complexity in quantum field theory, J. High Energy Phys. 10 (2017) 107.
[25] S. Chapman, J. Eisert, L. Hackl, M. P. Heller, R. Jefferson, H. Marrochio, and R. C. Myers, Complexity and entanglement for thermofield double states, SciPost Phys. **6**, 034 (2019).
[26] R. Khan, C. Krishnan, and S. Sharma, Circuit complexity in fermionic field theory, Phys. Rev. D **98**, 126001 (2018).
[27] A. Bernamonti, F. Galli, J. Hernandez, R. C. Myers, S.-M. Ruan, and J. Simón, First Law of Holographic Complexity, Phys. Rev. Lett. **123**, 081601 (2019).
[28] P. Caputa and J. M. Magan, Quantum Computation as Gravity, Phys. Rev. Lett. **122**, 231302 (2019).
[29] N. Chagnet, S. Chapman, J. de Boer, and C. Zukowski, Complexity for conformal field theories in general dimensions, arXiv:2103.06920.
[30] P. Caputa, N. Kundu, M. Miyaji, T. Takayanagi, and K. Watanabe, Liouville action as path-integral complexity: From continuous tensor networks to AdS/CFT, J. High Energy Phys. 11 (2017) 097.
[31] J. Boruch, P. Caputa, D. Ge, and T. Takayanagi, Holographic path-integral optimization, J. High Energy Phys. 07 (2021) 016.
[32] D. Carmi, R. C. Myers, and P. Rath, Comments on holographic complexity, J. High Energy Phys. 03 (2017) 118.
[33] A. Reynolds and S. F. Ross, Divergences in holographic complexity, Classical Quant. Grav. **34**, 105004 (2017).
[34] A. Akhavan and F. Omidi, On the role of counterterms in holographic complexity, J. High Energy Phys. 11 (2019) 054.
[35] F. Omidi, Regularizations of action-complexity for a pure BTZ black hole microstate, J. High Energy Phys. 07 (2020) 020.
[36] J. L. Cardy and D. C. Lewellen, Bulk and boundary operators in conformal field theory, Phys. Lett. B **259**, 274 (1991).
[37] D. M. McAvity and H. Osborn, Energy momentum tensor in conformal field theories near a boundary, Nucl. Phys. **B406**, 655 (1993).
[38] D. M. McAvity and H. Osborn, Conformal field theories near a boundary in general dimensions, Nucl. Phys. **B455**, 522 (1995).
[39] D. E. Berenstein, R. Corrado, W. Fischler, and J. M. Maldacena, The operator product expansion for Wilson loops and surfaces in the large N limit, Phys. Rev. D **59**, 105023 (1999).
[40] A. Kapustin, Wilson-'t Hooft operators in four-dimensional gauge theories and S-duality, Phys. Rev. D **74**, 025005 (2006).
[41] A. Karch and L. Randall, Locally localized gravity, J. High Energy Phys. 05 (2001) 008.
[42] O. DeWolfe, D. Z. Freedman, and H. Ooguri, Holography and defect conformal field theories, Phys. Rev. D **66**, 025009 (2002).
[43] D. Gaiotto and E. Witten, Supersymmetric boundary conditions in $N = 4$ super Yang-Mills theory, J. Stat. Phys. **135**, 789 (2009).
[44] K. Nagasaki and S. Yamaguchi, Expectation values of chiral primary operators in holographic interface CFT, Phys. Rev. D **86**, 086004 (2012).
[45] M. de Leeuw, C. Kristjansen, and K. Zarembo, One-point functions in defect CFT and integrability, J. High Energy Phys. 08 (2015) 098.
[46] I. Buhl-Mortensen, M. de Leeuw, C. Kristjansen, and K. Zarembo, One-point functions in AdS/dCFT from matrix product states, J. High Energy Phys. 02 (2016) 052.
[47] I. Buhl-Mortensen, M. de Leeuw, A. C. Ipsen, C. Kristjansen, and M. Wilhelm, One-Loop One-Point Functions in Gauge-Gravity Dualities with Defects, Phys. Rev. Lett. **117**, 231603 (2016).

[48] I. Buhl-Mortensen, M. de Leeuw, A. C. Ipsen, C. Kristjansen, and M. Wilhelm, A quantum check of AdS/dCFT, J. High Energy Phys. 01 (2017) 098.
[49] I. Buhl-Mortensen, M. de Leeuw, A. C. Ipsen, C. Kristjansen, and M. Wilhelm, Asymptotic One-Point Functions in Gauge-String Duality with Defects, Phys. Rev. Lett. **119**, 261604 (2017).
[50] M. de Leeuw, A. C. Ipsen, C. Kristjansen, K. E. Vardinghus, and M. Wilhelm, Two-point functions in AdS/dCFT and the boundary conformal bootstrap equations, J. High Energy Phys. 08 (2017) 020.
[51] S. Bonansea, S. Davoli, L. Griguolo, and D. Seminara, Circular Wilson loops in defect $\mathcal{N} = 4$ SYM: Phase transitions, double-scaling limits and OPE expansions, J. High Energy Phys. 03 (2020) 084.
[52] S. Komatsu and Y. Wang, Non-perturbative defect one-point functions in planar $\mathcal{N} = 4$ super-Yang-Mills, Nucl. Phys. **B958**, 115120 (2020).
[53] S. Bonansea and R. Sánchez, Wilson loops correlators in defect $\mathcal{N} = 4$ SYM, Phys. Rev. D **103**, 046019 (2021).
[54] S. Chapman, D. Ge, and G. Policastro, Holographic complexity for defects distinguishes action from volume, J. High Energy Phys. 05 (2019) 049.
[55] O. Aharony, O. DeWolfe, D. Z. Freedman, and A. Karch, Defect conformal field theory and locally localized gravity, J. High Energy Phys. 07 (2003) 030.
[56] Y. Sato and K. Watanabe, Does boundary distinguish complexities?, J. High Energy Phys. 11 (2019) 132.
[57] P. Braccia, A. L. Cotrone, and E. Tonni, Complexity in the presence of a boundary, J. High Energy Phys. 02 (2020) 051.
[58] R. Auzzi, S. Baiguera, S. Bonansea, G. Nardelli, and K. Toccacelo, Volume complexity for Janus AdS_3 geometries, J. High Energy Phys. 08 (2021) 045.
[59] M. Flory, A complexity/fidelity susceptibility g-theorem for $AdS_3/BCFT_2$, J. High Energy Phys. 06 (2017) 131.
[60] A. Bhattacharya, A. Bhattacharyya, P. Nandy, and A. K. Patra, Islands and complexity of eternal black hole and radiation subsystems for a doubly holographic model, J. High Energy Phys. 05 (2021) 135.
[61] D. Bak, M. Gutperle, and S. Hirano, A dilatonic deformation of AdS(5) and its field theory dual, J. High Energy Phys. 05 (2003) 072.
[62] D. Z. Freedman, C. Nunez, M. Schnabl, and K. Skenderis, Fake supergravity and domain wall stability, Phys. Rev. D **69**, 104027 (2004).
[63] E. D'Hoker, J. Estes, and M. Gutperle, Ten-dimensional supersymmetric Janus solutions, Nucl. Phys. **B757**, 79 (2006).
[64] A. B. Clark, D. Z. Freedman, A. Karch, and M. Schnabl, Dual of the Janus solution: An interface conformal field theory, Phys. Rev. D **71**, 066003 (2005).
[65] T. Takayanagi, Holographic Dual of BCFT, Phys. Rev. Lett. **107**, 101602 (2011).
[66] M. Fujita, T. Takayanagi, and E. Tonni, Aspects of AdS/BCFT, J. High Energy Phys. 11 (2011) 043.
[67] J. Estes, K. Jensen, A. O'Bannon, E. Tsatis, and T. Wrase, On holographic defect entropy, J. High Energy Phys. 05 (2014) 084.
[68] M. Gutperle and A. Trivella, Note on entanglement entropy and regularization in holographic interface theories, Phys. Rev. D **95**, 066009 (2017).
[69] I. Papadimitriou and K. Skenderis, Correlation functions in holographic RG flows, J. High Energy Phys. 10 (2004) 075.
[70] C. Bachas, J. de Boer, R. Dijkgraaf, and H. Ooguri, Permeable conformal walls and holography, J. High Energy Phys. 06 (2002) 027.
[71] M. Alishahiha, Holographic complexity, Phys. Rev. D **92**, 126009 (2015).
[72] R. Abt, J. Erdmenger, H. Hinrichsen, C. M. Melby-Thompson, R. Meyer, C. Northe, and I. A. Reyes, Topological complexity in AdS_3/CFT_2, Fortschr. Phys. **66**, 1800034 (2018).
[73] R. Auzzi, S. Baiguera, A. Legramandi, G. Nardelli, P. Roy, and N. Zenoni, On subregion action complexity in AdS_3 and in the BTZ black hole, J. High Energy Phys. 01 (2020) 066.
[74] M. Miyaji, T. Numasawa, N. Shiba, T. Takayanagi, and K. Watanabe, Distance between Quantum States and Gauge-Gravity Duality, Phys. Rev. Lett. **115**, 261602 (2015).
[75] C. A. Agón, M. Headrick, and B. Swingle, Subsystem complexity and holography, J. High Energy Phys. 02 (2019) 145.
[76] I. Affleck and A. W. W. Ludwig, Universal Noninteger 'ground state degeneracy' in Critical Quantum Systems, Phys. Rev. Lett. **67**, 161 (1991).
[77] D. Bak, M. Gutperle, and A. Karch, Time dependent black holes and thermal equilibration, J. High Energy Phys. 12 (2007) 034.